Robotic Crack Detection and Classification via AdaBoost-RVM Implementation

Yao Yeboah, Wei Wu, Wang Jun Jie, and Zhu Liang Yu
School of Automation Technology, South China University of Technology, Guangzhou, China
Email: yeboahjunior@yahoo.com

***Abstract*—This paper presents an automation approach towards the detection and classification of cracks on bridge surfaces using a robot platform. The approach is designed to exploit the physical features of cracks and is therefore capable of overcoming the challenges that traditional crack detection approaches are faced with. The approach adopts the Beamlet and Wavelet Transforms in the realization of a robust crack segmentation scheme. The Radon transform is coupled with the Projection Variance towards the extraction of crack features which facilitates a high specificity even in the presence of noise and texture irregularities. Finally, in order to render all this information useful and applicable towards the maintenance of bridges, a classification scheme is proposed which classifies cracks into non-crack, simple crack and complex crack categories. The classification scheme is realized through an AdaBoosted RVM implementation that achieves a high classification accuracy and generalization. This detection and classification system is deployed on the six-legged robot platform designed to operate semi-autonomously on bridges. The performance of this scheme is verified through comparison experiments with state-of-the-art and the experimental results indicate that the proposed scheme achieves effective results while outperforming some of the state-of-the art in terms of accuracy and classifier training time.**

***Index Terms*—crack detection, crack classification, AdaBoost-RVM, image processing**

I. Introduction

Bridges are designed to bear large traffic volumes and within the lifetime of a bridge, it is subject to cumulative damage from adverse weather conditions, drastic weather changes as well as the wearing effect of the motor vehicles that traverse almost incessantly in certain cases. The expiration of certain components of the bridge's structure could also compound and further escalate this degradation process. If left unchecked, this degradation results in a compromise of the integrity and load-bearing capacity of the bridge which could ultimately lead to a collapse. This bears strong economic implications and hence motivates the periodic inspection of bridges in an attempt to efficiently deduce their physical conditions and carry out necessary and timely maintenance operations. Such routine inspections and maintenance operations in themselves have posed life-threatening situations to maintenance personnel due to the locations and structures of most bridges. Machine vision and robotic vision have offered opportunities in the automation of these processes. Cracks are arguably one of the most important indicators of the physical integrity of bridges and tapping information from cracks has been the goal of most machine vision systems that have attempted to offer solutions within this problem domain. Through image preprocessing, segmentation and detection, traditional machine vision has attempted to offer solutions to this problem. The solutions are broadly categorized into online and offline approaches. While offline approaches have had no time constraints, they have had the advantage of relying on much denser computational mechanisms which have boosted their accuracies whereas in online approaches, time constraints are present and hence there is usually a trade-off between accuracy and processing time. Regardless which category of implementation is undertaken, crack detection and classification has been riddled with challenges that have stemmed from its reliance on machine vision. These challenges include but are not limited to uneven illumination, texture inhomogeneity on the bridge surface, low reflectivity in regions where cracks occur leading to a reduction in the intensity of crack pixels and hence, leading to a sharp contrast between crack and background pixels.

From a morphological point of view, cracks could be regarded as linear structures whose physical representations derive from the joint actions of the variations in the load that the bridge surface bears, as well as the uneven structural strength which results from the structural design.

II. Related Work

Regardless the application domain, all systems that attempt to extend machine and robotic vision towards inspection tasks can be broadly grouped and termed as Computer-aided Inspection. Computer-aided inspection has drawn considerable attention from the research community and its progress and evolution has been widely documented over the decade. Numerous surveys have covered the topic with some outstanding ones being seen in [1]-[5]. A key component of these systems is the approach they take towards imaging. While some implementations have relied upon depth imaging [6], others have continued to adopt intensity imaging due to its ease of implementation as well as its relatively lower

Manuscript received April 17, 2015; revised August 31, 2015.

doi: 10.18178/ijmerr.4.4.361-367

computational complexity, compared with range imaging. Intensity imaging algorithms have greatly relied upon various signal processing techniques which include but are not limited to Gabor Filters [7], morphological operations [8], [9] and the Wavelet Transform [10]-[12]. In [10], the Wavelet Transform is adopted in reducing the impact of noise while the Otsu thresholding is applied towards the segmentation of cracks. This approach proved effective in situations where noise was quite minimal, whereas performance became unstable with an increase in noise. This unstable performance is explained by the fact that the approach fails to take into account the physical features of cracks such as shape features which could offer increased robustness in segmentation. In a bid to boost segmentation performance, some algorithms have proposed to segment the frame itself in multiple smaller sized frames through implementation with a sliding window, after which crack segmentation is applied independently to each sub-frame. An example of such a segmentation scheme is seen in [13]. Generally speaking, segmentation performance is significantly higher in such schemes but performance is still far from ideal. The major drawback with such segmentation schemes is attributed to the fact that manual tagging of crack samples is usually required and this has the potential of introducing subjective errors into the overall performance. Henrique and Correia presented a crack identification scheme based on algebraic computation of probability in [14]. This approach was capable of accounting for the horizontal and vertical directions of cracks as well as their standard differential features. However, this scheme depended excessively on prior information which rendered it incapable of handling the various shapes that cracks could assume owing to its inability to guarantee generalization. Based on digital image processing techniques, another approach is presented in [15] towards surface distress detection in pavements. This approach also relied excessively on traditional image processing techniques while failing to incorporate robust features into its framework. All these approaches have shown effective performances as well as certain drawbacks that both merit further research and investigation.

Based directly upon the physical features of cracks, a crack detection and classification approach is proposed for implementation in automated bridge inspections

III. Automated Bridge Crack Detection and Classification

A. General Overview

The proposed approach discussed here in this paper is sub-divided into six computational stages as illustrated in Fig. 1.

The original colour images from the bridge surface are acquired by means of the single RGB camera mounted onboard the six-legged spider robot. Since the proposed approach makes no use of colour information, the image is converted to gray-scale and passed on to the preprocessing stage, stage 2. Taking into account that cracks manifest themselves within high-frequency regions in the image, the Fourier High-Pass and Gaussian High-Pass filters are applied in boosting the contrast and highlighting the cracks within the image while discarding lower frequency components in a discriminative manner. The Beamlet transform is at this point applied in the third stage towards a segmentation of cracks, based on the physical features of cracks. At the fourth computational stage, the Wavelet and Radon Transforms together with the Projection Variance are applied in extracting features that are representative of cracks and then passed along into stage 5 where classifier training is conducted. While we do not claim novelty in proposing the Adaboost-RVM classifier, the major contribution of this paper is its combination scheme between the AdaBoost and the RVM and also how the resultant AdaBoost-RVM is applied towards classifier training and classification in stages 5 and 6 respectively. In stage 6, crack images are classified into non-crack, linear and complex categories.

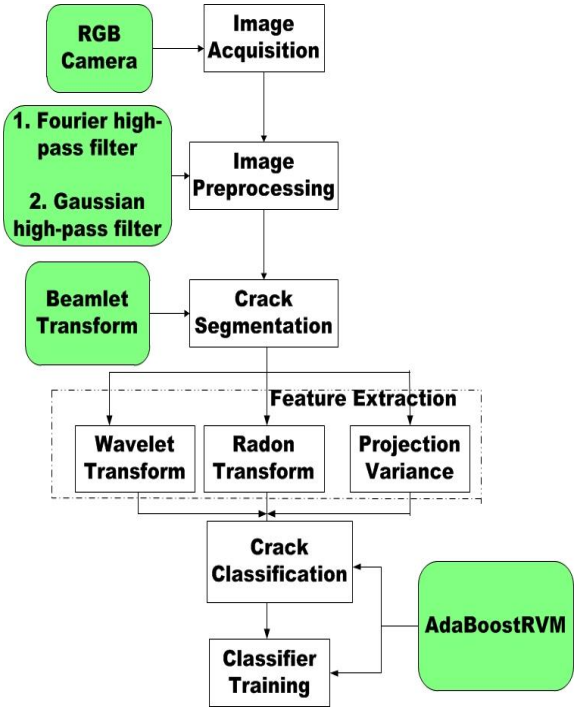

Figure 1. Flow chat illustration of the proposed scheme.

B. Image Acquisition

As illustrated in the Fig. 2, the entire bridge crack detection and classification system is implemented upon a six-legged spider robot. The entire platform is multidisciplinary and the scope of this paper will only be limited to the imaging, crack detection and crack classification components. The bridge surface images are acquired with and RGB camera that is mounted on the side of spider robot at an angle of 90° to the bridge surface. The position of the camera is selected, taking into the account the various gaits that the spider applies in movement so as not to occlude the surface of the bridge at any point in time. The acquired images from the camera are transferred to the onboard computing platform via an RS485 communication link. It is necessary to mention here that, in the paper, the bridge surface refers to both the top-facing and bottom-facing surfaces of the

bridge as the spider robot is equipped with suction cups, designed to enable it maneuver both on top and underneath the bridge.

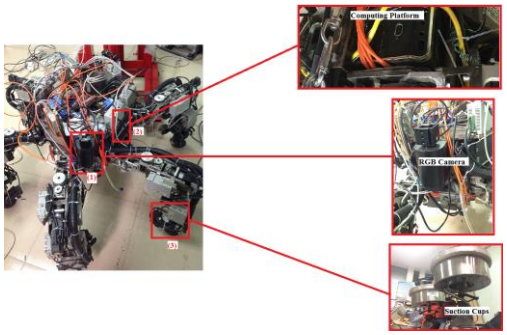

Figure 2. The image acquisition platform built upon the six-legged spider robot where: (1) RGB Camera; (2) Computer Platform Embedded into the robot; (3) Suction Cups equipped on each foot of the robot.

C. Image Preprocessing

The original input image acquired by the RGB camera is riddled with redundant and in some cases, information that bears no application potential. We treat all this information as noise and hence there is the need to remove them while also highlighting the crack information. First and foremost, the proposed algorithm has no need for the colour information which is present within the original image. The first stage in preprocessing is therefore to convert the original image into gray-scale. In order to highlight the crack information while dimming all other information, it is crucial to understand the physical nature of cracks and how they manifest within an image. Firstly, the gray values of cracks tend to be much higher than those of the surrounding pixels due to the sharp changes that occur at the boundaries where cracks connect with the rest of the image. It is therefore deducible that in the frequency domain, crack pixels should be positioned at relatively higher frequencies. This motivates our selection of the Fourier high-pass filter in the first preprocessing step. The effect of the filter is a sharpening of the image contrast and a highlighting of the cracks that may be present within the image. A feature of noise within the input image is a manifestation ringing or otherwise referred to as wavy effects within and around the central frequency region of the image. The second preprocessing stage therefore adopts the Gaussian high-pass filter which attenuates these central frequency components and further boosts the contrast of the input image.

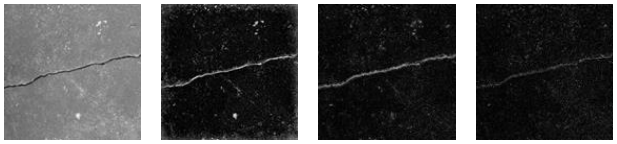

(a) (b) (c) (d)

Figure 3. Comparison of (a) the original image and Gaussian Filter output with (b) D0=0.002 , (c) D0=0.08, (d) D0=0.8

The quality of the Gaussian Filter output is strongly dependent on the Gaussian width parameter as well as its lower cutoff frequency, which we represent as D0. We establish this relation by presenting the original gray-scale image along with Gaussian filter results with some selected lower cutoff values shown in Fig. 3.

D. Crack Segmentation

The task of target segmentation is perhaps one of the most fundamental problems associated with machine vision. In adopting this machine vision technique towards crack detection, traditional approaches have essentially focused on gray threshold segmentation due to its implementation simplicity and high efficiency. However such approaches rely heavily upon local features in order to achieve the segmentation result and this has rendered them inefficient in the presence of significant amounts of noise. This limitation of gray threshold segmentation has been noted by recent literature that has attempted to propose solutions to the flaws existent in tradition techniques. Note-worthy attempts are seen in [10] and [13] where sliding windows are applied in sub-dividing the original image into sub-windows after which preprocessing of each sub-window is conducted, followed by the extraction of features for the training of neural networks towards the detection of cracks within each sub-window. Although such approaches have managed to overcome to some extent, the limitations of gray threshold segmentation, they fail to take into account the shape features of the cracks they attempt to detect and hence, in the presence of uneven illumination and complex background textures, segmentation performance rapidly deteriorates.

In this paper, the Beamlet transform is adopted towards the segmentation of cracks. The Beamlet transform was originally introduced as a multi-scale image analysis tool in [16]. The transform has been shown to have the capability of computing a line's position, direction and magnitude within an image while also being robust to noise. Given an nxn pixel image containing two points and a line segment, referred to as a beam, as illustrated in Fig. 4(a), dividing the image into $0 < m < \log_2 n$ sub-images yields $O(n^2 \log_2 n)$ beamlets as illustrated in Fig. 4(b).

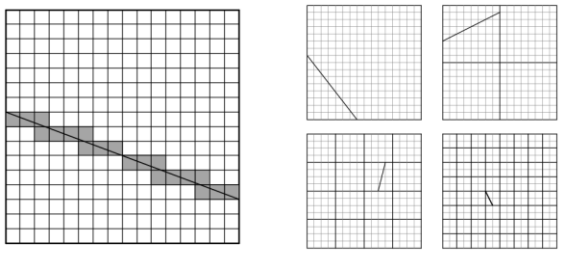

(a) (b)

Figure 4. (a) A beam through pixel points with their corresponding weights (b) Resulting beamlets of various scales and orientation.

The Beamlet transform function, T_f , of the 2-dimensional function, $f(x_1, x_2)$, is defined in [10] as:

$$T_f(b) = \int_b f(x(l))dl, b \in B_E \quad (1)$$

where B_E represents a collection of all present beamlets. In the context of digital images, the Beamlet transform is

defined as the line integral in the discrete domain. This is formulated as:

$$T(b) = \sum_{b} f(i_1, i_2)\phi(i_1, i_2) \quad (2)$$

where, $f(i_1, i_2)$ represents the gray values of the pixel (i_1, i_2), while $\phi(i_1, i_2)$ represents the weight of each pixel. The interested reader is referred to the original work in [16] for a much detailed discussion of the Beamlet transform.

After the image has been passed through the preprocessing phase, a threshold value is obtained for the extraction of the binary image. In order to cut down computational load and time, we adopt a fixed window size of 16x16 pixels in order to constrain the total number of beams for each image to a maximum of $O(n^2)$. The Beamlet transform is then applied to each 16x16 sub-window after which each sub-window's Beamlet maximum value is compared with the previously selected threshold value. Sub-windows that have maximum values larger than the threshold are retained while all others are discarded. In this manner, the beam lengths reflect the crack lengths within each sub-window. The selection of the threshold value is therefore crucial in determining the accuracy of the Beamlet crack segmentation. Fig. 5 presents segmentation results with different threshold values.

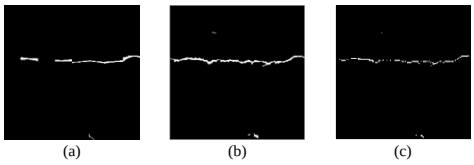

Figure 5. Beamlet Segmentation results with threshold values of (a) 3 (b) 5, (c) 7

E. Feature Extraction

Here in this paper, we assume that cracks assume irregular physical representations and are composed by a linear combination of pixels. The irregularities present within the physical structures of cracks make it possible to apply the Wavelet transform towards the extraction of representative features. As earlier stated, the pixels that make up cracks are linearly connected and this establishes a premise for the adoption of the Radon transform, coupled with the Directional Projection Variance in extracting features that establish the direction of cracks within the target image. This proposed feature extraction scheme is illustrated in Fig. 6.

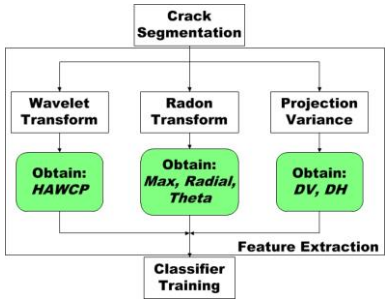

Figure 6. Crack feature extraction scheme.

In our feature extraction scheme, firstly, a two-dimensional scaling function is applied to the gray-scale image, represented as f(x,y). A one-dimensional Discrete Wavelet Transform (DWT) is then computed for the resulting image, column by column. Through an iteration of this decomposition process, a multi-scale Wavelet transform is achieved. The percentage of high-amplitude wavelet coefficients (HAWCP) within the image represents the total number of pixels present within a sub-band. It is represented as:

$$HAWCP = \frac{\sum_{p=0}^{W/8}\sum_{q=0}^{L/8}}{(\frac{W}{8}\cdot\frac{L}{8})} \quad (3)$$

where W and L represent the width and length of the gray-scale image respectively. The three-dimensional wavelet coefficient modulus can be obtained through a computation of the standard deviation of the wavelet coefficients. This computation can be obtained as

$$M_3(p,q) = \sqrt{HL_3^2(p,q) + LH_3^2(p,q) + HH_3^2(p,q)} \quad (4)$$

The Radon transform [17] has proven highly efficient in the extraction of linear features. Due to linear combination of pixels that make up cracks, the transform is applicable towards the extraction of crack features. The Radon transform along a line can be represented as

$$Rf(\alpha, s) = \int_{-\infty}^{+\infty} f((t\sin\alpha + s\cos\alpha), (-t\cos\alpha + s\sin\alpha))dt \quad (5)$$

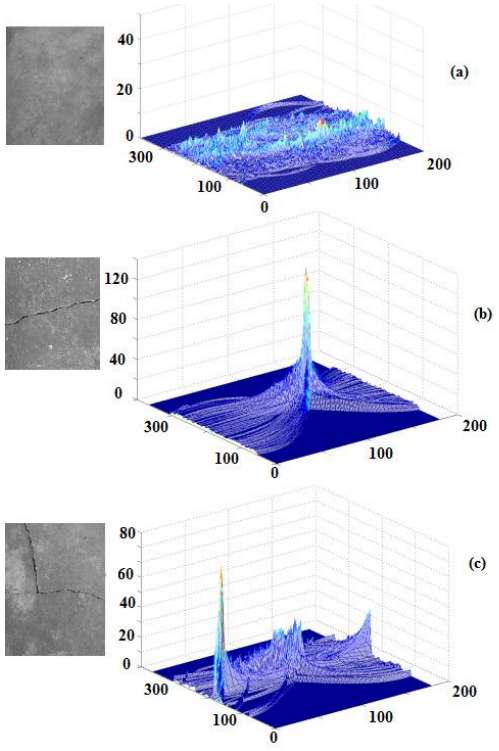

Figure 7. Radon transform results of (a) a sample without cracks (b) a sample with a simple crack, (c) a sample with a complex crack.

After applying the Radon transform to the gray-scale image, peak values are obtained in regions of the image where linear features are present. The corresponding α and s represent the direction and position of these features

within the image. We establish this relationship between the Radon transform and cracks in the Fig. 7.

Finally, at the feature extraction phase, the projection variance is applied. The projection variance has the capability of providing information on the position of the crack within the image, in relation with the horizontal and vertical axes. The projection variance along the horizontal and vertical axes are respectively formulated as:

$$D_H = \frac{1}{\mathrm{N}}\sum_{y=1}^{N}\left(I_H(y) - \frac{1}{\mathrm{N}}\sum_{y=1}^{N} I_H(y)\right)^2 \quad (6)$$

$$D_V = \frac{1}{\mathrm{N}}\sum_{x=1}^{N}\left(I_V(x) - \frac{1}{\mathrm{N}}\sum_{x=1}^{N} I_V(x)\right)^2 \quad (7)$$

The two parameters, D_H and D_V represent the rate of change of the crack along the horizontal and vertical axes respectively. Here also, we establish this relationship between cracks in the image and their projection variance. This relationship is illustrated in Fig. 8.

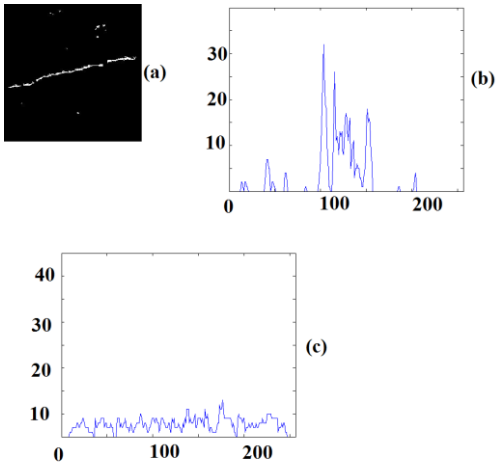

Figure 8. Establishing the relationship between cracks in (a) the gray-scale image and the projection variance along (b) the horizontal direction and (c) the vertical direction.

In Fig. 8, the projection variance of a gray-scale image with a single crack is computed. Due to the direction in which the crack is inclined, it is seen that the projection variance in the horizontal direction has sharply rising peaks while the corresponding vertical projection variance exhibits no such significant peaks.

Since in this paper, we attempt to not only detect cracks within the bridge surface images but to also classify these images into categories namely non-cracks, simple cracks and complex cracks, we establish the relationship between the features we extract at this stage and the three categories into which images will be classified. Towards achieving this, 90 bridge surfaces image samples are collected and manually labeled. The samples are collected such that there are 30 sample images for each of the three categories. The features presented in Fig. 6 are computed for all image samples and the average results are presented in Table I.

TABLE I. ESTABLISHING THE RELATIONSHIP BETWEEN THE EXTRACTED FEATURES AND CRACKS WITHIN THE SAMPLE IMAGES.

Feature Vector	Samples		
	Non Crack	Simple Crack	Complex Crack
HAWCP	0.4052	1.072	1.1258
Max	12.8904	71.6273	89.0890
Radial	0.3597	0.3842	0.2643
Theta	0.6278	0.9778	0.5889
DH	1.2563	71.3544	27.6186
DV	1.2625	2.3975	31.9323

F. Classifier Training

In this paper, cracks are classified into three categories based on the physical features of the crack. In order to achieve such a multi-class classification scheme, we adopt and implement an Adaboost-RVM classifier. Some literature [18]-[20] have presented implementation schemes in which the SVM has been applied towards distinguishing defects from pseudo-defects in steel structures. Compared with the SVM, the RVM possesses a high generalization capability which enables it to more effectively identify and classify samples for which it has not yet been trained. This inspires our selection of the RVM for our application since the bridge surface presents a broad spectrum of surface textures. Attempting to train a classifier for all texture possibilities could increase the training and classification times, thereby adversely affecting the online performance of the algorithm.

The Adaboost algorithm originally proposed in [21] offers a scheme in which the RVM classifier can be boosted quite efficiently due to the simple interface of the RVM classifier itself. Adaboost requires no prior knowledge nor learning process and this signifies that boosting is achievable without a trade-off between classification accuracy and training time. The scheme through which a combination between the RVM and AdaBoost is achieved is as follows.

- Given a training set, $\{(\mathrm{x}_i, \mathrm{y}_i)\}_{i=1}^{N}$,where $y_i \in \{-1,1\}$, assign a label x_i to the correct class.
- Assign the initial distribution of the training set:
$$D_1(\mathrm{i}) = \frac{1}{N}$$
- Train the RVM classifier: $h_t : X \to \{-1,1\}$ with $t = 1,2,3,...,T$.
- Compute the errors of the distribution D_t of the RVM classifier:
$$\varepsilon_t = P_{D_t}(h_t(x_i) \neq y_i) = \sum_{i=1}^{N} D_t(i)(h_t(x_i) \neq y_i) .$$
- Compute the weight of the RVM classifier:
$$\alpha_t = \frac{1}{2}\ln\left(\frac{1-\varepsilon_t}{\varepsilon_t}\right)$$
- Update the training set: $D_{t+1}(i) = \frac{D_t(i)\exp(-\alpha_t y_i h_t(x_i))}{Z_t}$; where Z_t represents the normalized constant.
- Enhance the classifier through: $H(x) = sign(\sum_{t=1}^{T}\alpha_t h_t(x))$

Once this Adaboosted RVM multi-class classifier has been achieved, non-cracks, simple cracks and complex cracks are labeled as $\{x_i^A\}_{i=1}^n$, $\{x_i^B\}_{i=1}^n$ and $\{x_i^C\}_{i=1}^n$ respectively with corresponding class labels of A, B and C.

IV. Experimental Results

Experiments are conducted with the six-legged robot on actual bridge surfaces in an attempt to evaluate the online performance of the proposed approach. The robot platform was deployed to acquire 200 bridge surface images. Out of the total 200 sample images acquired, manual labeling established that 92 were non-crack samples, 76 contained simple cracks and the remaining 32 contained complex cracks.

A cross validation is conducted with another 100 samples for each training and testing instance. The images were acquired in RGB at a resolution of 256x256. The algorithm testing results are presented in Table II. In order to validate the efficiency and accuracy of the proposed approach, a comparison is conducted with Adaboost, RVM, BP Neural Network and Prior Mathematical Modeling.

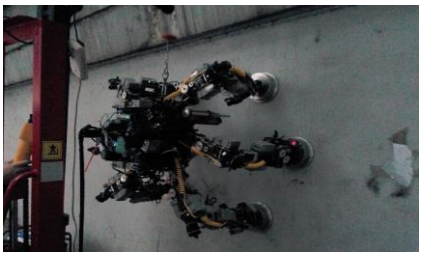

Figure 9. The six-legged spider is deployed on actual bridge surfaces in order to acquire image samples for the validation of the performance of the proposed classification approach.

TABLE II. Evaluation Results of the Proposed AdaBoost-RVM Classification Approach for Bridge Crack Samples.

Testing Instance	Accuracy (%)	Processing Time (s)	Weak Classifiers
1	93.5	32.3	3
2	95.1	35.6	4
3	94.7	36.4	3

TABLE III. Evaluation Results of the Proposed AdaBoost-RVM Classification Approach in Comparison with Some State-of-the-Art

Classifier	**Accuracy (%)**	**Training Time (s)**	**Processing Time (s)**
Adaboost	87.8	643.4	24.5
RVM	83.7	71.8	5.3
BP Neural Network	88.5	1.022.4	34.7
Prior Mathematical Modeling	82.1	-	5.6
Proposed Approach	94.8	713.8	26.7

To the best of our knowledge, at the time of these experiments, there are still no conventional datasets available for bridge crack classification and hence, these comparison experiments are conducted with images that are acquired with the six-legged robot platform as illustrated in Fig. 9. A total of 200 images are applied in these validation experiments and the results are presented in the Table III.

V. Conclusions

In this paper, a crack detection and classification scheme is presented for the application of bridge maintenance. The proposed approach is implemented on a six-legged spider robot which is designed to operate semi-autonomously on bridge surfaces. Although crack detection and classification is a well studied area and the Adaboost-RVM has been applied to this problem prior to this paper, this paper addresses the problem by presenting a new way by which crack features can be extracted through the Wavelet and Radon transforms as well as the projection variance. This paper also discusses the topic of crack detection and classification on bridges using actual images captured by the spider robot while maneuvering the bridge surface. This allows for a practical presentation and discussion of the problem as well as the challenges that accompany deployment. The presented classification scheme is tested in experiments and the obtained results have shown that the approach performs efficiently with a high classification accuracy and a low processing time. This confirms that indeed this approach is feasible in applications that require real-time classification of cracks. The proposed approach in this paper is also compared with state-of-the-art. This comparison is conducted on real images acquired by the spider robot. Comparison results have shown that the approach achieves a significantly higher accuracy in classification compared with state-of-the-art. While the training and processing times are slightly higher in some cases, the overall processing time is still small enough, making this approach applicable in real-time applications. The high accuracy in classification that the proposed approach achieves is attributed to the crack detection and segmentation schemes that take into account the physical features of cracks

References

[1] R. T. Chin and C. A. Harlow, "Automated visual inspection: A survey," *IEEE Trans. on Pattern Analysis and Machine Intelligence*, vol. PAMI-4, pp. 557-573, Nov. 1982.

[2] J. B. C. Eduardo, "Review of automated visual inspection 1983-1993, Part I: Conventional approaches," *SPIE*, vol. 2055, pp. 128-158, 1993.

[3] J. B. C. Eduardo, "Review of automated visual inspection 1983-1993, Part II: Approaches to intelligent systems," *SPIE*, vol. 2055, pp. 159-172, 1993.

[4] S. N. Timothy and K. J. Anil, "A survey of automated visual inspection," *Computer Vision and Image Understanding*, vol. 61, pp. 231 - 262, 1995.

[5] N. M. Elia, G. M. P. Euripides, Z. Michalis, P. Laurent, and D. L. Jean, "A survey on industrial vision systems, applications and tools," *Image and Vision Computing*, vol. 21, pp. 171-188, 2003.

[6] A. Landstrom and M. J. Thurley, "Morphology-based crack detection for steel slabs," *IEEE Journal of Selected Topics in Signal Processing*, vol. 6, pp. 866-875, Nov. 2012.

[7] J. P. Yun, S. H. Choi, B. Seo, C. H. Park, and S. W. Kim, "Defects detection of billet surface using optimized gabor filters," in *Proc. World Congress*, South Korea, 2008, pp. 77-82.

[8] M. R. Yazdchi, A. G. Mahyari, and A. Nazeri, "Detection and classification of surface defects of cold rolling mill steel using morphology and neural network," in *Proc. International Conference on Computational Intelligence for Modelling Control Automation*, 2008, pp. 1071-1076.
[9] D. Lee, Y. I. Kang, C. Park, and S. Won, "Defect detection algorithm in steel billets using morphological top-hat filter," in *Proc. Automation in Mining, Mineral and Metal Processing*, Vienna, 2009, pp. 209-212.
[10] E. Salari and G. Bao, "Pavement distress detection and classification using feature mapping," in *Proc. IEEE International Conference on Electro/Information Technology*, 2010, pp. 1-5.
[11] P. Y. Jong Y. Pil, C. Sung Hoo, J. J Yong, C. C. Doo, and W. K. Sang, "Detection of line defects in steel billets using undecimated wavelet transform," in *Proc. International Conference on Control, Automation and Systems*, Seoul, 2008, pp. 1725-1728.
[12] J. J. Yong, P. Y. Jong, S. H. Choi, and W. K. Sang, "Defect detection algorithm for corner cracks in steel billet using discrete wavelet transform," in *Proc. ICCAS-SICE*, Fukuoka, 2009, pp. 2769-2773.
[13] X. Guoai, M. Jianli, L. Fanfan, and N. Xinxin, "Automatic recognition of pavement surface crack based on BP neural network," in *Proc. International Conference on Computer and Electrical Engineering*, Phuket, 2008, pp. 19-22.
[14] H. Oliveira and P. L. Correia, "Automatic road crack detection and characterization," *IEEE Trans. on Intelligent Transportation Systems*, vol. 14, pp. 155-168, March 2013.
[15] A. Ouyang, C. Luo, and C. Zhou, "Surface distresses detection of pavement based on digital image processing," in *Proc. Computer and Computing Technologies in Agriculture IV*, Normal, IL, 2011, pp. 368-375.
[16] D. L. Donoho and X. Huo, "Beamlets and multiscale image analysis," in *Multiscale and Multiresolution Methods*, T. J. Barth, T. Chan, and R. Haimes, Eds., Springer, 2002, pp. 149-196.
[17] J. Radon, "On the determination of functions from their integral values along certain manifolds," *IEEE Trans. on Medical Imaging*, vol. 5, pp. 170-176, Dec. 1986.
[18] P. Y Jong, H. P. Chang, B. H. Moon, H. Hwawon, and C. Seho, "Vertical scratch detection algorithm for high-speed scale-covered steel BIC (Bar in Coil)," in *Proc. International Conference on Control Automation and Systems*, Gyeonggi-do, 2010, pp. 342-345.
[19] C. C. Doo, J. J. Yong, P. Y. Jong, W. Y. Sung, and W. K. Sang "An algorithm for detecting seam cracks in steel plates," *World Academy of Science, Engineering and Technology*, vol. 6, pp. 1459-1462, 2012.
[20] J. J. Yong, C. Sung Hoo, P. Y. Jong, P. Chang Hyun, and W. K. Sang, "Detection of scratch defects on slab surface," in *Proc. 11th International Conference on Control, Automation and Systems*, Gyeonggi-do, 2011, pp. 1274-1278.
[21] F. Yoav and E. S. Robert, "A decision-theoretic generalization of on-line learning and an application to boosting," *Journal of Computer and System Sciences*, vol. 55, pp. 119-139, 1997.

Yao Yeboah received the B.Eng. in the field of electronic information engineering from the Huazhong University of Science and Technology, Wuhan, China in 2011 and the M.Eng. from the South China University of Technology, Guangzhou, China in 2013. He is currently pursing his Ph.D. in the Department of Electrical and Computer Engineering, School of Automation Science and Engineering, South China University of Technology. His research interests include pattern recognition, intelligent systems and robotic vision.

Wei Wu received the Ph.D. degree in the field of control theory and control engineering from the Huazhong University of Science and Technology, Wuhan, China in 2000. He is currently a professor in the School of Automation Science and Engineering of South China University of Technology, Guangzhou, China. His research interests include intelligent control systems, robotic control and engineering, pattern recognition and intelligent systems.

Wang Junjie received the M.Eng. in control theory and control engineering from the South China University of Technology, Guangzhou, China in 2013. His research interests include machine learning, artificial intelligence and machine vision for robotic applications.

Zhu L. Yu received the BSEE in 1995 and the MSEE in 1998, both in electronic engineering from the Nanjing University of Aeronautics and Astronautics, Nanjing, China and the Ph.D. in 2006 from Nanyang Technological University, Singapore. He joined the Center for Signal Processing, Nanyang Technological University in 2000 as a research engineer, then as a Group Leader. In 2008, he joined the College of Automation Science and Engineering, South China University of Technology, China. He was promoted to be a full Professor in 2009. His research interests include signal processing, machine learning, computer vision and applications in biomedical engineering and robotics.